

BOX TRUSS DEVELOPMENT

AND

ITS APPLICATIONS

J. V. Coyner

Martin Marietta Denver Aerospace
Denver, Colorado

Large Space Antenna Systems Technology - 1984
December 4-6, 1984

TOPICS FOR DISCUSSION

Since 1977, Martin Marietta Denver Aerospace has aggressively pursued development of deployable structural systems applicable to a wide variety of Shuttle-transportable large space system requirements. This effort has focused on the deployable box truss, mechanisms and materials development, mesh reflector design and fabrication, gate frame truss design and fabrication, and offset-fed antenna design and analysis.

Figure 1 lists the activities that will be discussed in this paper.

- o BOX TRUSS DESIGN
- o MECHANISM AND MATERIALS DEVELOPMENT
 - METAL MATRIX COMPOSITE COMPONENTS
 - PRECISION JOINTS
 - ENHANCED PASSIVE DAMPING DESIGNS
- o MESH REFLECTOR DEVELOPMENT
- o GATE FRAME TRUSS FOR SOLAR ARRAYS
- o INTEGRATED OFFSET-FED ANTENNA SYSTEM
 - 15-METER SPINNING RADIOMETER
 - 60-X 120-METER PUSH BROOM RADIOMETER

Figure 1

SUMMARY OF LSS ACTIVITY

Each year significant steps were taken in the maturity of the box truss design and the understanding of the supporting analysis. Figure 2 summarizes the evolution of the deployable box truss and related technology activities. During 1977 and 1978, the emphasis was placed on design and analytical verification of the box truss structure performance. During 1979, 1980, and 1981, design refinements and hardware fabrication were directed towards GFRP integration with primary emphasis on low cost. This activity culminated in the fabrication and demonstration of the 4.6-meter cube. During 1982, a full-scale prototype of a gate frame truss was fabricated and tested. Also, a mesh test model was fabricated to validate the mesh reflector analytical tools and to demonstrate fabrication techniques. During 1983 and 1984, mesh analytical work continued, metal matrix composite development made significant progress, precision joint designs were fabricated and demonstrated, and passive damping augmentation concepts were developed. During 1985, a mesh reflector will be integrated to the 4.6-meter cube, and dynamic testing of a 20-meter truss will be performed.

- 1977
 - O BOX TRUSS DESIGN CONCEIVED ON IR&D
 - O DESIGN DEVELOPED AND ANALYZED ON "ON-ORBIT ASSEMBLY" PROGRAM
 - O SINGLE-FRAME DEMONSTRATION MODEL FABRICATED
- 1978
 - O DESIGN AND FABRICATION OF SINGLE-FRAME PROTOTYPE STRUCTURE (GFRP TUBES AND METALLIC FITTINGS)
- 1979
 - O DESIGN REFINEMENT INTEGRATING LOW-COST GFRP FITTINGS AND MEMBERS
- 1980
 - O DESIGN OF GFRP 4.6-METER BOX TRUSS CUBE
 - O FABRICATION OF ALL COMPONENTS
- 1981
 - O ASSEMBLY AND TEST OF 4.6-METER CUBE
- 1982
 - O MESH MODEL FABRICATION AND TEST
 - O ASSEMBLY AND TEST OF GATE FRAME TRUSS
- 1983
 - O METAL MATRIX COMPONENT DESIGN, FABRICATION, TEST
 - O PRECISION JOINT DESIGN, FABRICATION, TEST
- 1984
 - O METAL MATRIX COMPONENT DESIGN, FABRICATION, TEST
 - O MESH TIE SYSTEM ANALYTICAL DEVELOPMENT
 - O PASSIVE DAMPING COMPONENT DEVELOPMENT
- 1985
 - O MESH INTEGRATION TO 4.6-METER CUBE
 - O DYNAMIC TEST OF STATICALLY DETERMINATE AND INDETERMINATE TRUSSES

Figure 2

FULL-SCALE PROTOTYPE CUBE

During 1980, the design of each of the box truss components was reviewed and redesigned to achieve maximum weight, cost, and thermal stability while meeting the stowed, deploying, and deployed structure requirements. A prototype was made for each component and tested to verify manufacturing methods (feasibility and tolerance manageability) and stiffness, strength, and weight. By the end of 1980, all components for a full-scale prototype 15-ft, deployable box truss cube were completed and assembly had started. Final assembly was completed in 1981. Figure 3 shows the resulting prototype cube in a deployed and stowed configuration, respectively. Summarized below are the design features of the full-scale prototype cube:

4.6m deployable cube

Stows in 0.3m square by 4.6m long (0.15m per module)

- 36 modules (28m x 28m deployed) stow in 1m by 1m by 4.6m

All GFRP except for hinge pins and springs

High performance (high stiffness, low CTE)

Low weight - 27 kg

High accuracy - better than 0.1mm on all axes

50 N diagonal pretension

Exhibits ideal truss characteristics found in all box truss systems

- Purity of load paths, i.e., no bending moments in deployed structure

All components and members fully constrained when stowed

Every corner fitting stabilized by bonded interface to vertical tube

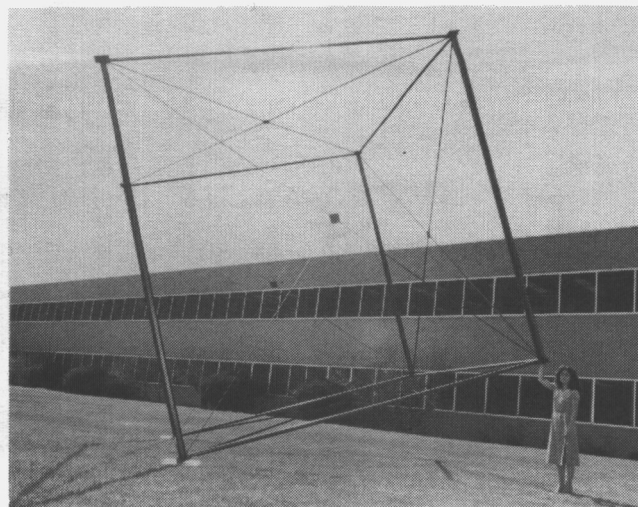
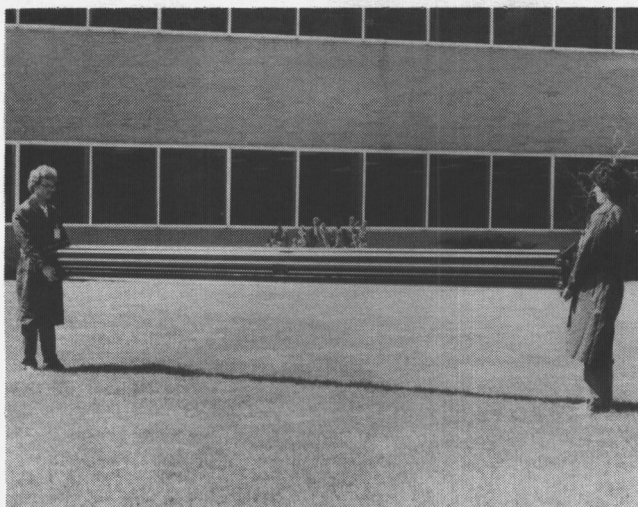


Figure 3

METAL-MATRIX COMPOSITE COMPONENT DEVELOPMENT

Metal-matrix composites combine some of the best attributes of the resin matrix composites and the conventional metallic materials. Some of their major advantages over Gr/E are high resistance to laser and radiation damage, good thermal and electrical conductivity, no outgassing in the space thermal-vacuum environments and potential for automated fabrication. These composites offer higher specific modulus and a lower coefficient of thermal expansion than conventional metallic alloys. Our applications development in the use of metal-matrix composites is broadening and is reflected in the generation of basic material and design data.

Figure 4 summarizes the materials being developed and the parts being fabricated and tested.

o WHY METAL MATRIX COMPOSITES

- HIGH RESISTANCE TO THERMAL DISTORTION (ZERO CTE)
- HIGH SPECIFIC STIFFNESS
- HIGH CONDUCTIVITY

o MATERIALS BEING DEVELOPED

- GRAPHITE MAGNESIUM
- GRAPHITE ALUMINUM
- SIC ALUMINUM

o PARTS BEING FABRICATED AND TESTED

- MEMBER END FITTINGS
- TRUSS NODE FITTINGS
- MEMBERS WITH VARIOUS CROSS SECTIONS (TUBE, SQUARE, CHANNEL, L, ROD)

Figure 4

Gr/Al and Gr/Mg TRUSS MEMBERS

Continuous reinforced metal-matrix composites are reinforced by long continuous fibers unidirectionally or in crossplied configurations. Among the present systems boron/aluminum composites have been used for the Space Shuttle orbiter and a few other aerospace applications. However, their use has been extremely limited because of poor fabricability. To alleviate this problem, graphite-reinforced aluminum and magnesium alloys were developed and are ready to be used in space structures. Both Gr/Al and Gr/Mg composites offer excellent material properties for space applications; however, only Gr/Mg composites have the potential to achieve zero CTE.

Continuous Gr/Mg and Gr/Al are commonly produced by hot-pressing and diffusion-bonding the precursor wires to the face sheets. Although the process has produced some excellent products, forming complex shapes from flat products could present some material integrity problems. As a result, other processes such as pultrusion have been developed. Unidirectionally reinforced round or other symmetrical cross sections in Gr/Mg and Gr/Al have been successfully produced by pultrusion.

Gr/Mg components can also be produced by casting technology because of the recent development of wettable air-stable coatings. This definitely adds a greater dimension to the fabrication of Gr/Mg structures. Unfortunately, casting technology cannot now be applied to Gr/Al composites because of the lack of a suitable fiber coating.

Figure 5 is an example of Gr/AL pultrusion tube that was fabricated.

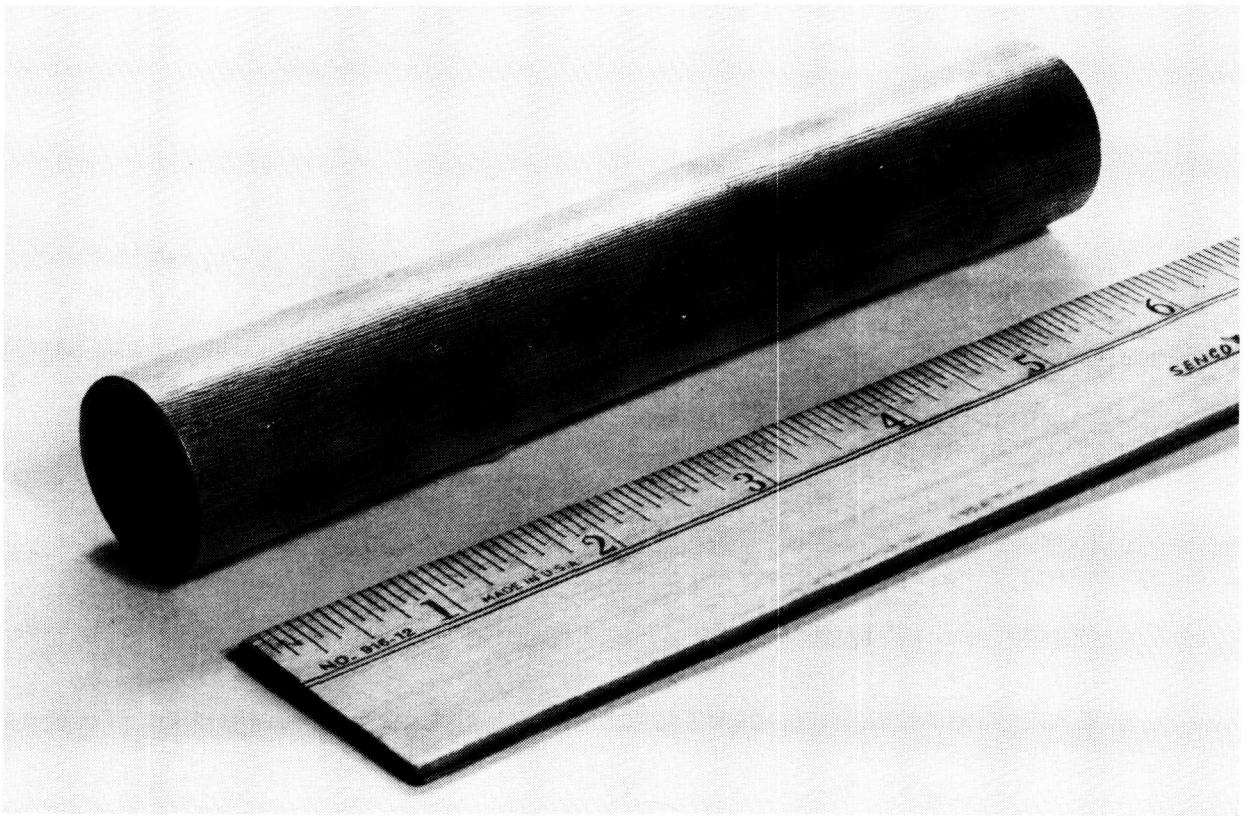


Figure 5

SiC/Al FITTING DEVELOPMENT

Metal-matrix composites are generally classified by two categories -- discontinuous reinforced, and continuous reinforced. Discontinuous reinforced metal-matrix composites are reinforced by chopped fibers, whiskers or particulates. Most advanced systems in this category are SiC whisker- or particulate-reinforced aluminum and magnesium alloys; of these SiC/Mg offers higher specific stiffness and a slightly lower CTE than SiC/Al. However, SiC/Mg is still regarded as a developmental material and many fabrication questions must be answered before its application. On the other hand, SiC/Al composites are well developed in almost every phase of materials technology, including material properties and primary and secondary fabrication processes.

SiC whisker- or particulate-reinforced aluminum alloys are commonly produced by powder metallurgy techniques. The manufacturing processes have been developed to the point that high-quality products are produced with good interfacial bonds and low hydrogen pickup. Material properties close to the analytically predicted values are being realized.

SiC/Al composites can be fabricated in various shapes using such conventional processes for aluminum alloys as forging, extrusion sheet metal-forming machine, and mechanical joining. The only area of some concern could be the welding technology because porosity is sometimes observed in the fusion zone. Extensive Martin Marietta Aerospace experience in welding SiC/Al has produced welded products of the highest quality.

Figure 6 shows examples of 2 different types of SiC/Al fittings fabricated by Martin Marietta.

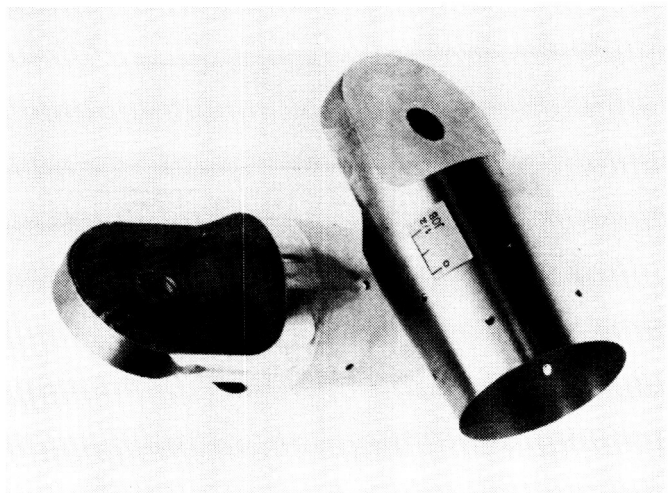
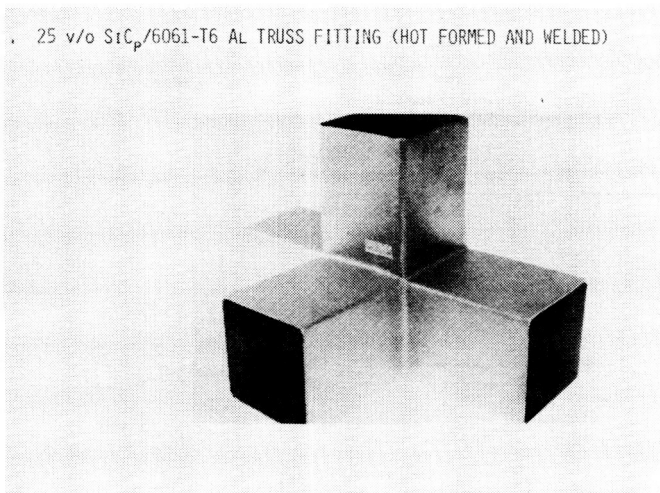


Figure 6

PRECISION JOINT DESIGN AND FABRICATION

Three types of precision joints were designed, fabricated and tested to demonstrate their function and performance (precision tightening pin joints, precision 180-degree hinged joint and precision sliding joint).

The primary design requirements were:

1. Zero freeplay when in the fully deployed condition
2. Zero, or near-zero, coefficient of thermal expansion (CTE) through the joint
3. Continuity of stiffness through the joint
4. Manufacturing processes amenable to low-cost, low-volume production

Other design considerations included:

1. Long-term material stability in the space environment
2. Damping of deployment and other induced vibration
3. Thermal and electrical conductivity through the joints

Shown in Figure 7 are the design concepts fabricated and tested.

PRECISION SLIDING JOINT DESIGN

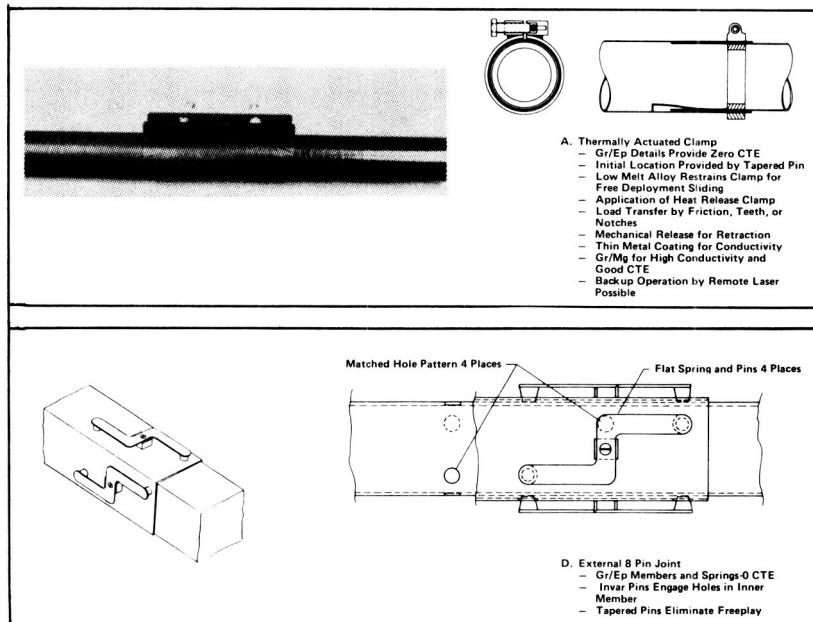
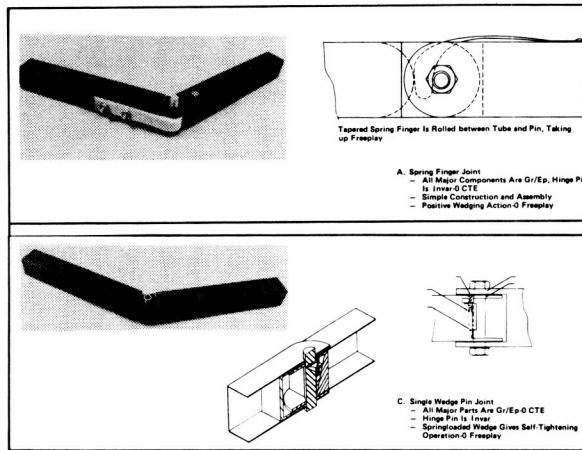


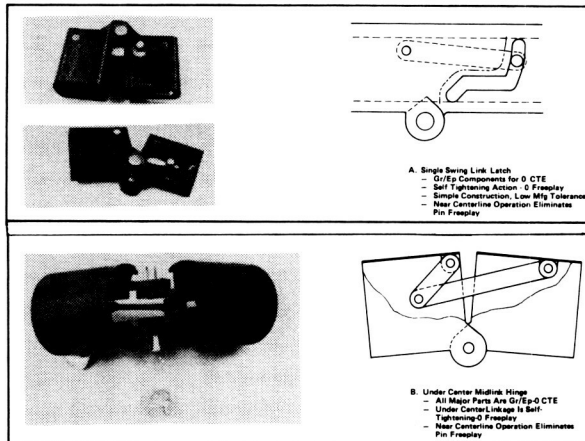
Figure 7

PRECISION JOINT DESIGN AND FABRICATION (CONTINUED)

PRECISION TIGHTENING PIN JOINT DESIGN



PRECISION 180-DEGREE HINGED-JOINT DESIGN



PRECISION 180-DEGREE HINGED-JOINT DESIGN

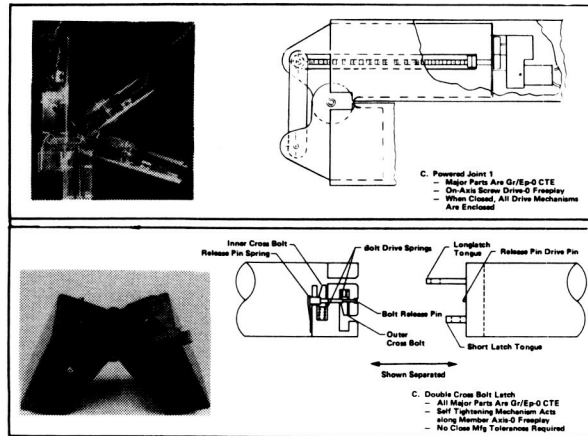


Figure 7 (Concluded)

ENHANCED PASSIVE DAMPING DESIGNS

Future large space systems will be required to slew rapidly, point accurately, and focus electromagnetic radiation with great dimensional precision while subjected to a variety of environmental and on-board excitations. The success with which these requirements can be met depends largely on system damping (traditionally assumed to be 1% or less). Consequently, elaborate and expensive active control systems may be required to provide additional damping. An alternate means of increasing system damping is to add passive mechanical damping.

The ultimate objective of the Passive and Active Control of Space Structures (PACOSS) program is to develop new and possibly unconventional design procedures to apply viscoelastic damping treatments that, in concert with state-of-the-art active attitude, figure control, active vibration suppression, and other passive damping schemes, can be extended to the development of military large space systems (LSS) with a high level of confidence.

Martin Marietta has constructed two ground test articles being submitted to vibration testing (shown in the left side of Figure 8). The size of the articles relates to a generic large space structure. A damper mechanism is shown in the right side of Figure 8.

The truss articles being tested are called space age tuning forks, and vibrations are created to determine their ability to dampen. The vibration is 1 Hz, and damping is being increased to 3.8% headed toward 6% damping. Eventually, an advanced damping system is expected to function at 10%.

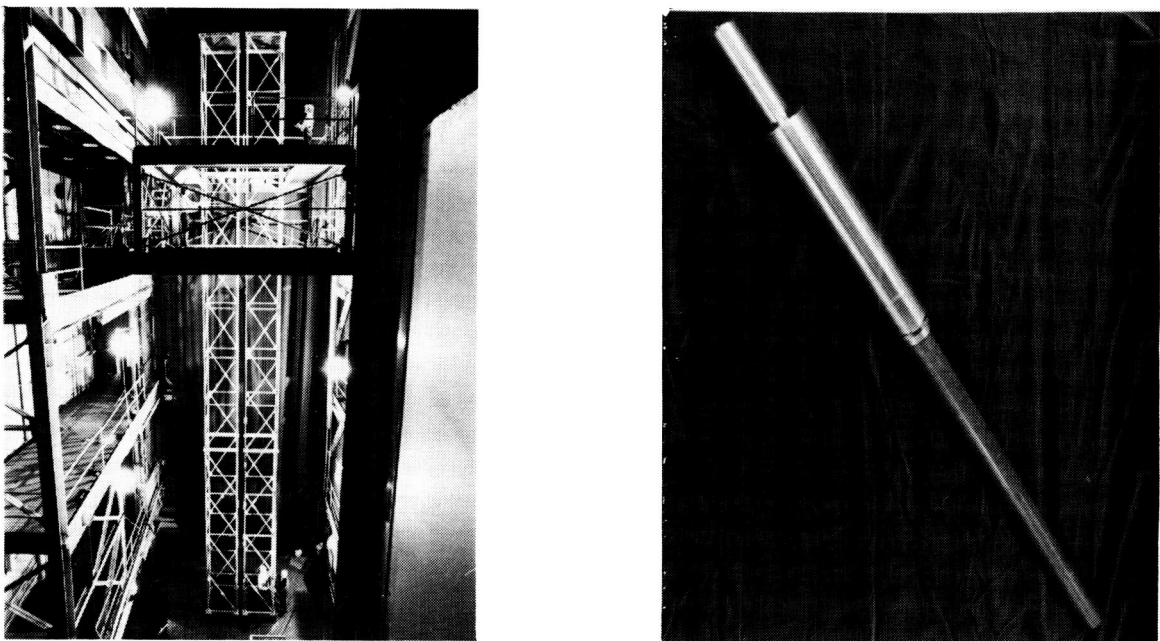


Figure 8

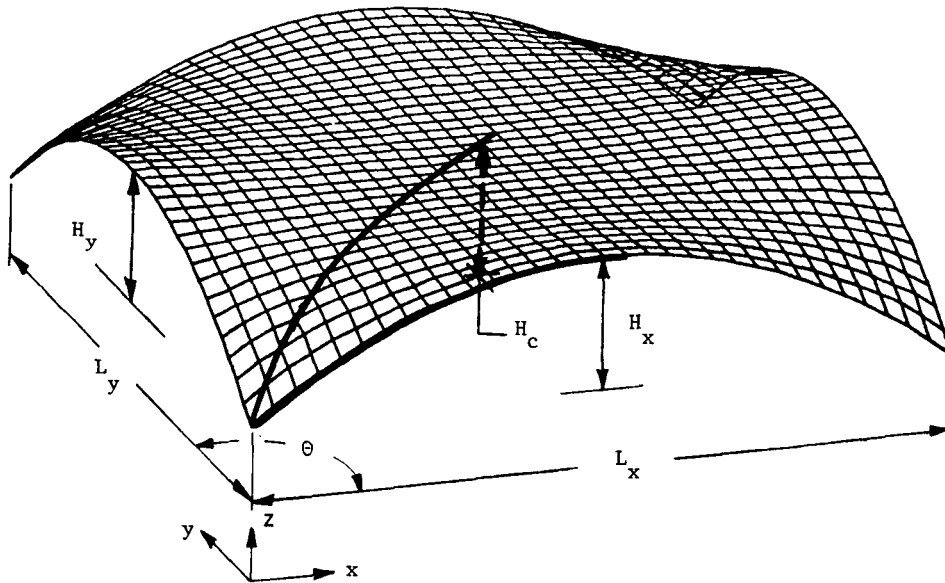
REFLECTOR MESH ANALYSES

The capability to analyze the response of mesh reflectors supported and shaped by a tie-cord system has been developed. A very accurate reflective surface is vital to the performance of LSS antennas. The present design of the reflective surface uses a gold reflective mesh supported and shaped by a tie-cord system made up of either graphite or quartz.

A user-friendly and cost-effective mesh analysis method was developed that was directed specifically at the LSS reflector design problems. Pre- and post-processors were tailored for LSS configuration to reduce the cost of the analysis. Analysis technique included rapid methods for optimizing a particular design (e.g., permitting the analyst or designer to change material properties such as coefficient of thermal expansion (CTE) to represent on-orbit adjustment techniques. Accurate determination of these various disturbances to the reflective surface geometry required the use of non-linear stress-stiffened finite-element (FE) techniques. Stress stiffening, also known as tension stiffening, is the increase in lateral stiffness of a structural element due to the increase in positive axial strain (tension) in the element. Cost-effective algorithms were developed because existing FE programs, such as ANSYS, which have stress stiffening capabilities, are in such generalized form that the analysis is both time consuming and costly.

Figure 9 shows a typical computer-generated mesh pillow.

RESULTS MESH SURFACE DESIGN



- MESH PILLOW SHAPE MEASURED FROM MESH PILLOW MODELS FABRICATED UNDER IRAD D-54D
- INPUT TO EMPIRICAL EQUATION
 - TIE CORD SPACING L_x AND L_y
 - HEIGHT OF PILLOW IN CENTER H_c
 - HEIGHT OF PILLOW AT CENTER OF EACH EDGE H_x AND H_y
- EMPIRICAL EQUATION FORM

$$(0 \leq \theta \leq 45) z = F(H_c, H_x, L_x, x, \theta)$$

$$(45 \leq \theta \leq 90) z = F(H_c, H_y, L_y, y, \theta)$$

Figure 9

MESH PILLOW TEST MODEL

An IR&D activity was initiated to design and understand a parabolic mesh reflector. This activity included fabrication of mesh models and surface distortion measurements. The shape of the reflective surface using the double-catenary cord system is defined by several factors: mesh tension and compliance, upper surface cord pattern (spacing), tension and stiffness, drop-cord stiffness and length, rear-cord stiffness and length, and local radius of curvature. Further, geometric saddling effects (pillowing) due to biaxial tensioned mesh and the upper surface cord pattern cause local deformations. Figure 10 (upper) shows a scale test model of a reflector surface. Measurements were made to determine pillow shape versus mesh tension and cord tension. When the panel's shape is duplicated and scaled to a mesh surface on a 15-meter reflector with an 11.94-meter focal length and average drop-cord spacing of 42.8 cm, the rms surface errors (best-fit mesh saddles relative to the ideal parabola) are 0.020 cm, and the worst-case deflections (drop-cord attachment points) are 0.067 cm behind the ideal parabola. Assuming 1/40 of a wavelength can be assigned to rms mesh distortions, the mesh surface design proposed would be appropriate for frequencies of 11 GHz. A smaller mesh test model (Figure 10, lower) was used to determine the optimum surface-cord tension for a mesh tie system.

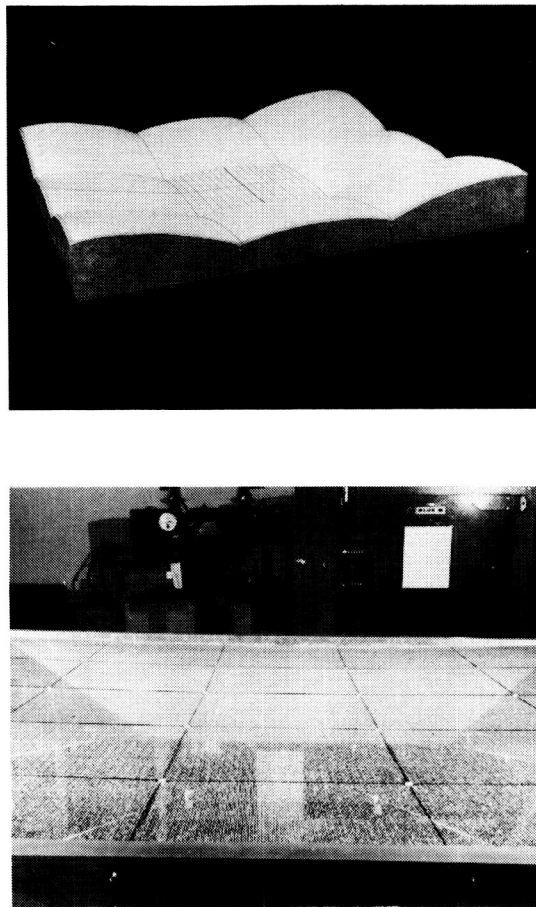


Figure 10

GATE FRAME TRUSS FOR SOLAR ARRAYS

The gate frame truss (shown in Figure 11) that was developed to provide deployment and support for antenna array panels also has excellent potential for supporting solar array panels and blankets. The gate frame truss design was applied to improving the dynamic characteristics of the 25-kw NASA solar array and to provide a large solar array that can be packaged in one orbiter. The results of the study showed that for the 25-kw solar array, by replacing the lattice mast with a gate frame truss, a factor of 8 improvement in dynamics is realized. For the large solar array design, a 600-ft x 50-ft solar array was achieved in a single orbiter. This provides a 300-kw solar array assuming 10 watts/ft² power output. The 300-kw solar array also had the necessary volume and mass available in the orbiter for all subsystems to provide a complete free-flyer spacecraft.

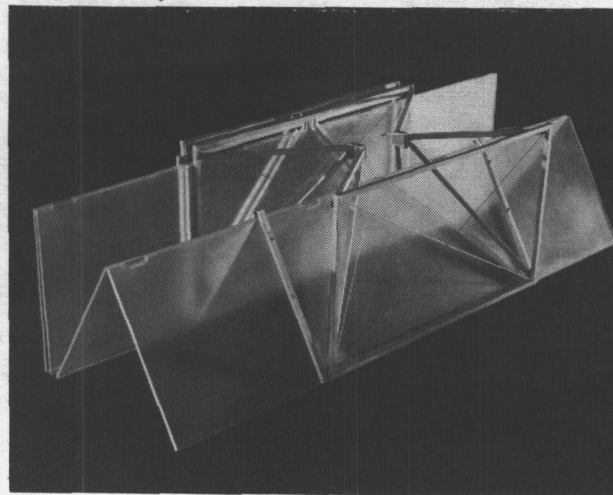
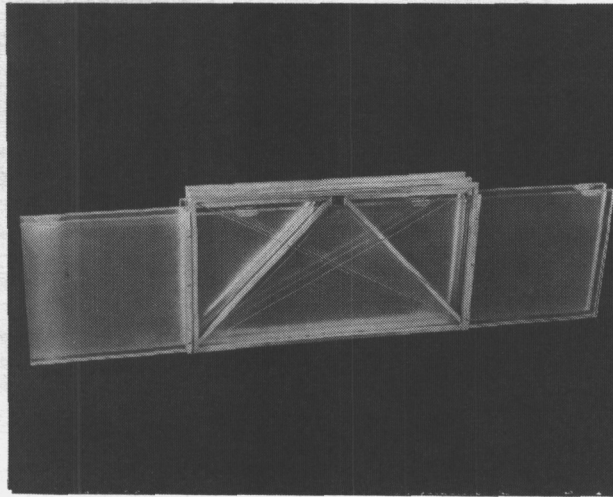


Figure 11

FULL-SCALE GATE FRAME TRUSS MODEL

Figure 12 shows the full-scale single-box prototype of a gate frame truss that was fabricated and tested.

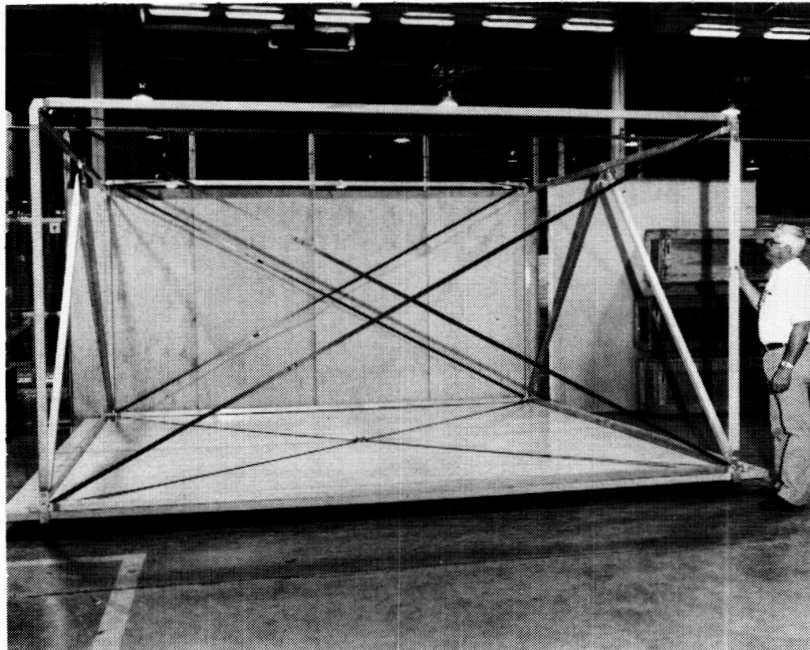
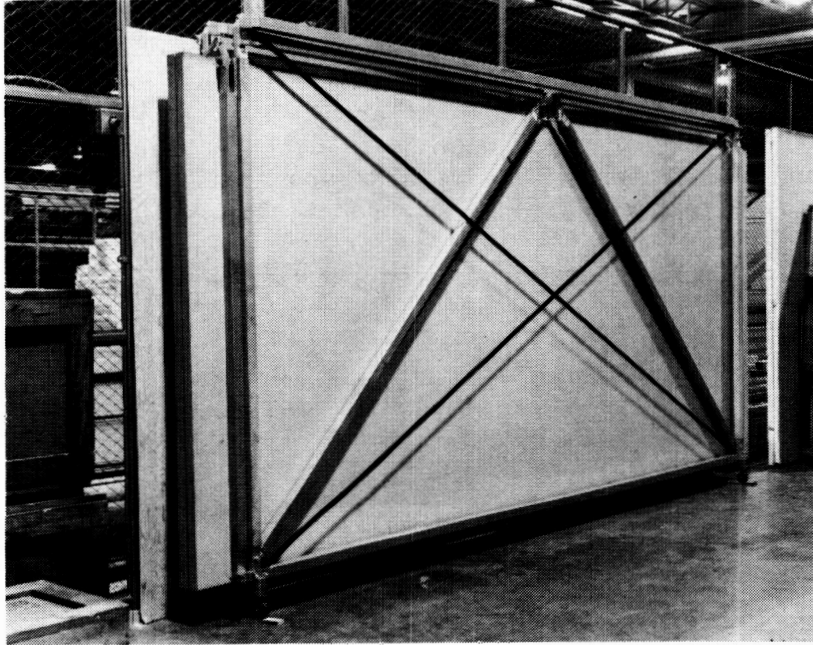


Figure 12

15-METER BOX TRUSS REFLECTOR WITH INTEGRATED FEED MAST*

A unique deployable feed mast has been developed for the offset feed space deployable antenna. The novel feature of this design is that it uses an extension of the reflector truss structure rather than adding appendages. The design features efficient stowage, simple integration to the reflector structure, excellent thermal stability, light weight, and very high stiffness and dynamic stability. These features are achieved by using the efficiency and features of a deep truss structure. Previous offset feed masts were appendages added to the reflector structure and had less efficient packaging, more difficult integration, and substantially lower dynamic stability. Because of the high strength and stiffness, this mast can easily accommodate the more complicated and massive advanced feeds (e.g., line feeds, array feeds, and multi-frequency multi-beam feeds). A study was performed which required a 15-meter antenna with a deployed structural frequency of 12 Hz. This was easily achieved with the integrated offset feed mast. The results are summarized in Figure 13.

* Work performed under Contract NAS5-26496.

ANTENNA PERFORMANCE SUMMARY

0 REFLECTOR DIAMETER, M	15.0
0 FOCAL LENGTH, M	11.94
0 REFLECTOR AND FEED SUPPORT MAST, KG	400.0
0 FEED MASS ALLOCATION, KG	27.1
0 BALLAST MASS, KG	22.7
0 DEPLOYED FREQUENCY, HZ	
MODE 1	12.35
MODE 2	12.75
MODE 3	13.19
0 STOWED ENVELOPE, M	3.84 DIA X 4.47
0 STOWED FREQUENCY, HZ	17.2
0 SURFACE ACCURACY (RMS) WORST-CASE, CM	0.097
0 FEED LOCATION ACCURACY (AXIAL), CM	0.024
(CENTRIFUGAL CORRECTED)(LATERIAL), CM	0.051

Figure 13

DEPLOYMENT SEQUENCE

The structure is deployed in a controlled sequence of steps. Feed beams are deployed one cube at a time, and trusses are deployed one row of cubes at a time. In the latter case, the steps are accomplished in a preselected sequence with flat, cylindrical, and parabolic trusses, and virtually any beam shape.

As shown in Figures 14 and 15, the feed mast flips up first, after which the boxes on either side of the super box deploy outward. The bays on either side of the middle-deployed three are then deployed. Following this sequence, an entire row of five bays is deployed outward away from the feed mast. This is followed by each row deploying outward until the antenna support structure is fully self-deployed. The feed mast will then deploy its three boxes upward for the completion of the entire sequence. The deployment is controlled by latches between the cube-corner fittings. These latches release by remote control in proper sequence, initiating deployment of each section of the antenna support structure. The sequential nature of the deployment energy is an incremental manner, thereby reducing the possibility of producing structural failure in the deploying truss.

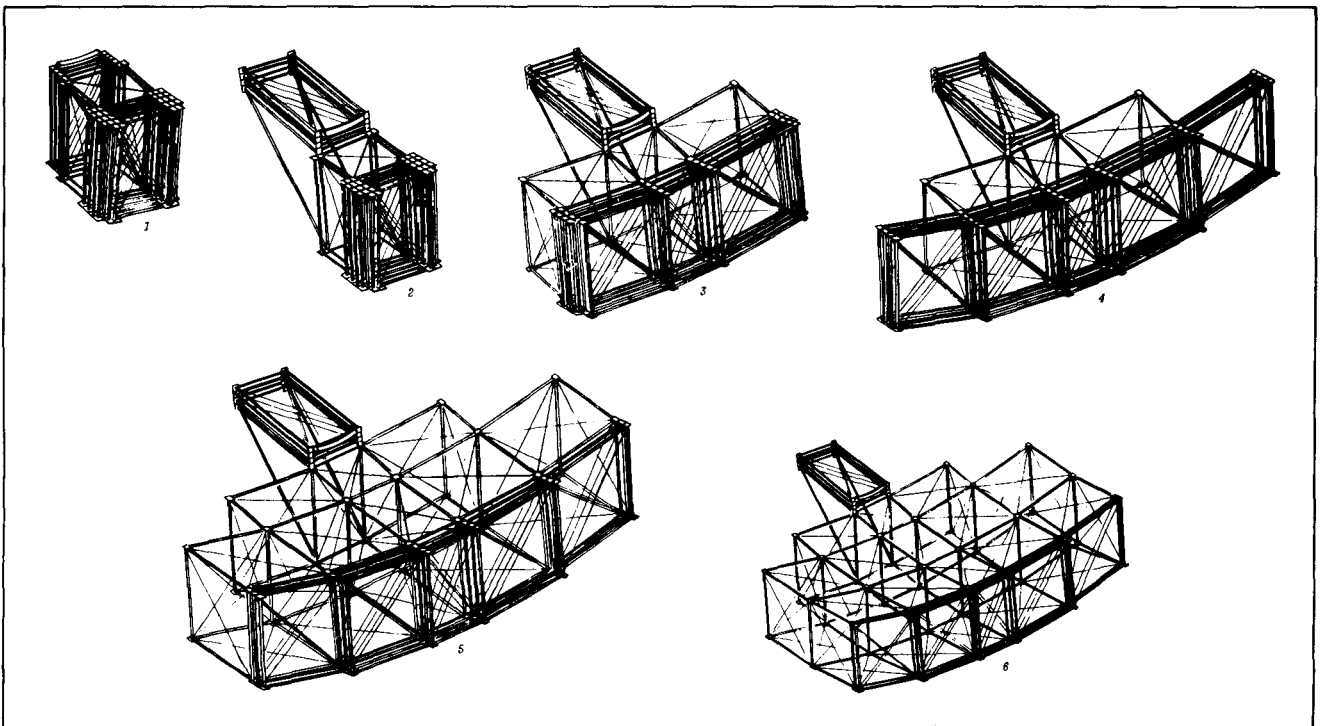


Figure 14

DEPLOYMENT SEQUENCE - COMPLETION

Figure 15 shows the completion of the reflector deployment and the full feed mast deployment. Total deployment of the reflector and feed mast (10 steps) takes approximately 5 minutes.

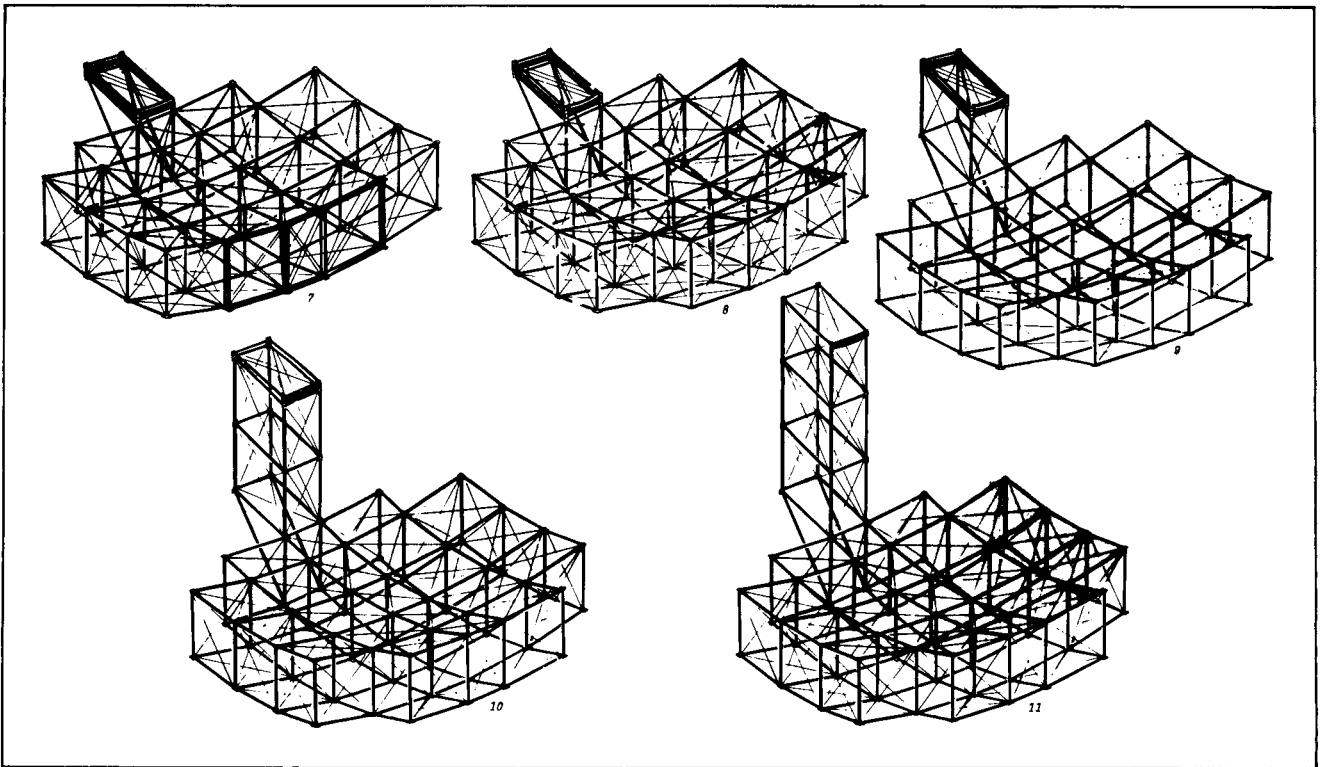


Figure 15

60- BY 120-METER RADIOMETER SPACECRAFT*

The 60- by 120-m Earth observation spacecraft (EOS) shown in Figure 16 is designed using the deployable box truss structure to form both the parabolic dish and feed mast. The structure easily stows within the orbiter bay. The 4-bay by 8-bay antenna support structure has an extremely high stiffness-to-weight ratio. The structure is made thermally stable by using low coefficient of thermal expansion (CTE) graphite/epoxy composite layups. The dynamic stability created by integration of the feed mast and antenna support structure is the basis for the high 1.08-Hz fundamental frequency of this structure. The key feature of this unique design is that the feed support mast is an extension of the reflector truss structure rather than an added appendage. This design features efficient stowage, simple integration with the reflector structure, excellent thermal stability, light weight, and very high stiffness and dynamic stability. These features are directly attributable to the efficiency and features of a deep truss structure.

* Work performed under Contract NAS1-16756.

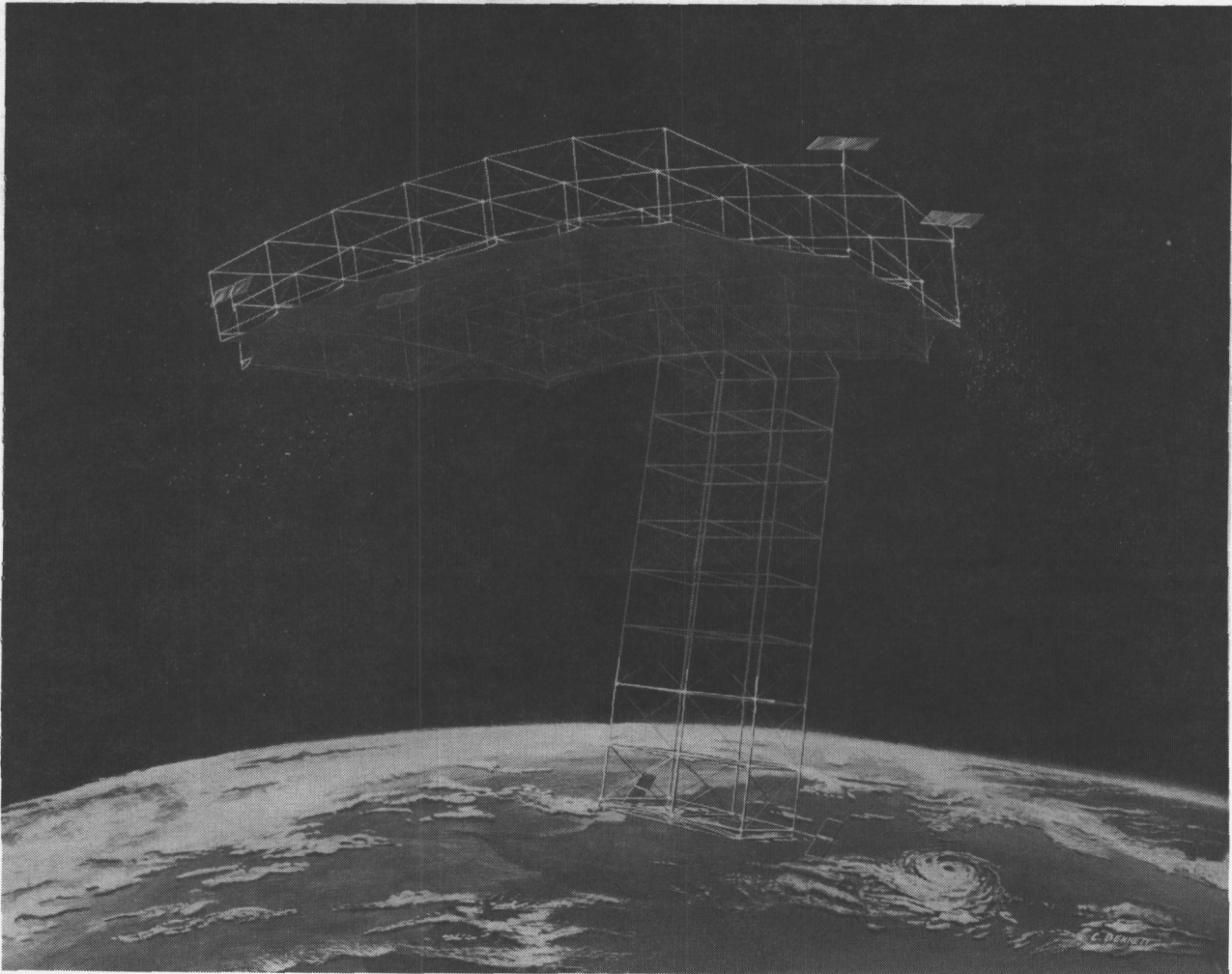


Figure 16

RADIOMETER SATELLITE SUBSYSTEM SUMMARY

Figure 17 summarizes the system and subsystem performance for the EOS radiometer satellite. The results indicate that the integrated offset mast box truss design produces a rigid and stable base for the large microwave radiometer and its ancillary sensors and subsystems. Higher structural frequencies reduce the potential for control instabilities and ensure that the dynamic response to the environmental forcing functions will be relatively small.

STRUCTURE

- 120M X 60M OFFSET LINE FED RADIOMETER
- 30M FEED ARC BOOM LOCATED 116.1M ABOVE SURFACE ON THE FOCAL AXIS
- BOX TRUSS, 15M BOXES SKEWED TO MEET PARABOLIC SHAPE (VERTICALS ALWAYS PARALLEL)
- STRUCTURE IS PARABOLIC IN BOTH DIRECTIONS - PARABOLIC CIRCULAR SHAPE ACHIEVED WITH STANDOFFS
- GRAPHITE MEMBERS AND CORDS
- STOWED VOLUME 4.25M X 17.8M
- SPHERICAL RADIUS 234.8
- TOTAL SYSTEM MASS 7635 KG
- FUNDAMENTAL DYNAMIC MODE 1.09 HZ

Frequency, GHz	Ground Resolution, km		Maximum No. Horns	Swathwidth, km
	Optimistic	Conservative		
1.4	2.95	14.75	58	173
5.5	0.88	4.5	90	350
10.68	0.41	2.06	88	18

- GOLD-PLATED MOLYBDENUM TRICOT KNIT MESH, 5.5 ENDS PER CM - ON 2M STANDOFFS
- F/D = 2, 58M EFFECTIVE APERTURE

Figure 17

MASS PROPERTIES FOR EOS SPACECRAFT

Figure 18 summarizes the mass properties of the EOS spacecraft. Notice that the total structural weight (60-120m reflector and 116m feed mast) was only 2769 kg. The structure supported 4866 kg of payload and still had excellent dynamic characteristics.

DYNAMIC ANALYSIS

Subsystem	Unit	Mass, kg/Unit	Total, kg
Feed Boom System	1	717	717
Electronics (GN&C, Communications & Data Processing)	1	110	110
Atmospheric Sounding Radar	1	70	70
Mesh and Tie System	6750 m ²	0.044	297
Science Pallet (SAR & Structure)	1	169	169
Twin PPTs	4	84	336
Single PPT	4	44	176
Power			
- Solar Panels	6	50	300
- Battery Packs	6	90	540
Orbit Transfer System			
- Inboard Propulsion System	2	325	650
- Outboard Propulsion System	2	118	236
Slewing Propulsion System	4	316	1265
Total Subsystem Mass			4866
Structural System			
Cube Corner Fitting			
- Full	67	0.479	32
- 3/4	52	0.332	17
- 1/2	20	0.222	4
Midlink Hinge	231	0.452	104
Mesh Standoff	42	0.8976	38
Structural Members			2574
Total Structure Mass			2769
Total Spacecraft Mass*			7635

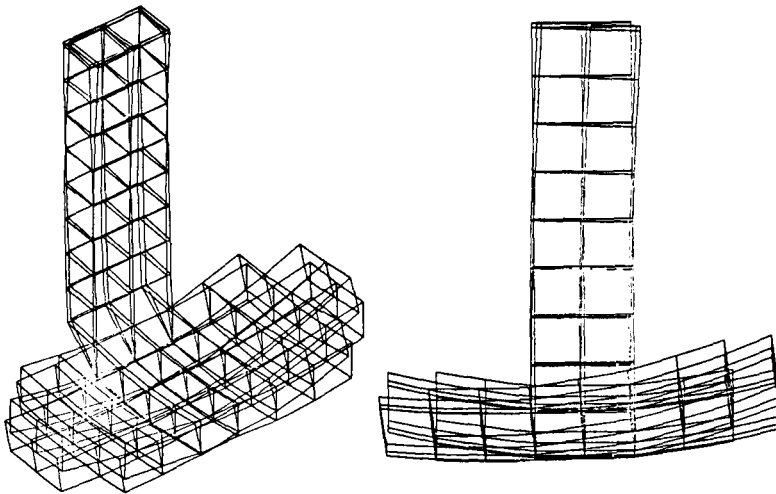
*With slewing and orbit transfer.

- MASSES OF VARIOUS SUBSYSTEMS AND STRUCTURAL COMPONENTS WERE LUMPED AT THE NODES
- MIDLINK HINGES, FEED BEAM, PROPELLANT MASSES WERE DISTRIBUTED ALONG THEIR RESPECTIVE MEMBERS
- THREE MASS CASES WERE ANALYZED FOR EOS

Figure 18

DYNAMIC ANALYSIS OF EOS SPACECRAFT

Figure 19 summarizes the dynamic performance of the EOS spacecraft. The fundamental frequency was 1 Hz which is 10 to 1000 times higher than other types of offset-fed parabolic antenna systems of similar size.



- FIRST MODE SHAPE (1.09 HZ) OF EOS W/O SLEWING OR ORBIT TRANSFER PROPELLANT
- BY MAXIMIZING STIFFNESS, THE CONTROL SYSTEM CAN BE SIMPLIFIED

Mode	Mass, kg		
	Without Slewing/ Orbit Transfer, Hz	With Slewing/ Orbit Transfer, Hz	With Slewing/ Orbit Transfer, Hz
1	1.09	0.911	0.711
2	1.13	0.963	0.736
3	1.14	0.969	0.766
4	1.32	0.972	0.782
5	1.38	0.990	0.844
6	1.39	0.998	0.900
MASS	5547	6812	7635

Figure 19